

The correlation averaging of a regularly arranged bacterial cell envelope protein

by W. O. SAXTON and W. BAUMEISTER*, *High Resolution Electron Microscope, University of Cambridge, Free School Lane, Cambridge CB2 3RQ*, and **Institut für Biophysik und Elektronenmikroskopie der Universität Dusseldorf Moorenstrasse 5, D-4000 Dusseldorf 1, West Germany*

KEY WORDS. Correlation averaging, crystal distortions, resolution assessment, symmetry assessment, cell envelopes, regular proteins.

SUMMARY

An adaptation of the 'correlation averaging' method is described which allows reliable and almost fully automatic image averaging in the case of near-periodic structures notwithstanding the presence of substantial crystal imperfections; methods for assessing resolution and symmetry without reliance on crystallinity are also discussed. Electron micrographs of negatively stained and rotary shadowed preparations of the HPI-layer protein from the cell envelope of *Micrococcus radiodurans* have been averaged using the method, and the projected structure is described to a resolution of about 1.9 nm.

INTRODUCTION

It has been apparent for some time that one of the factors limiting the resolution attainable by conventional image averaging of biological specimens is the limited size of the crystalline areas (natural or synthetic) available for reconstruction. The single-particle 'correlation averaging' methods developed by Frank and his co-workers (Frank *et al.*, 1978; Saxton & Frank, 1977) have permitted useful averaging without dependence on crystallinity, but the processing involved is necessarily much more tedious. In view of the large numbers of macromolecular specimens in which a basically crystalline structure is degraded by long- or short-range imperfections of various kinds, adaptation of the correlation averaging method to the near-periodic case (Saxton, 1980; Frank & Goldfarb, 1980; Frank, 1980), which simplifies it substantially, is obviously attractive in principle; in practice we have found the result to be not merely of more general applicability but also more convenient and reliable than the conventional methods relying on perfect crystallinity, and we would recommend it as a preferable alternative to these even for perfectly crystalline specimens. Accordingly, this paper explains the procedures we have adopted, discusses related problems of symmetry and resolution assessment when crystallinity can no longer be assumed, and indicates the principal considerations relevant to a comparison between the new and the conventional methods.

The structure of regular bacterial surface layers has become of some general interest now that it has transpired that such layers are more common than was anticipated even a few years ago (see, for example, Sleytr, 1978); their function is largely a matter of speculation however. We examine here the hexagonally packed intermediate (HPI) layer of the cell envelope of *Micrococcus radiodurans* (Kubler & Baumeister, 1978); this is typical of many such layers in that although the sheets isolated by detergent extraction contain as much as 50% of the entire cellular complement, giving little hope for the isolation of larger crystals, the maximum size of a

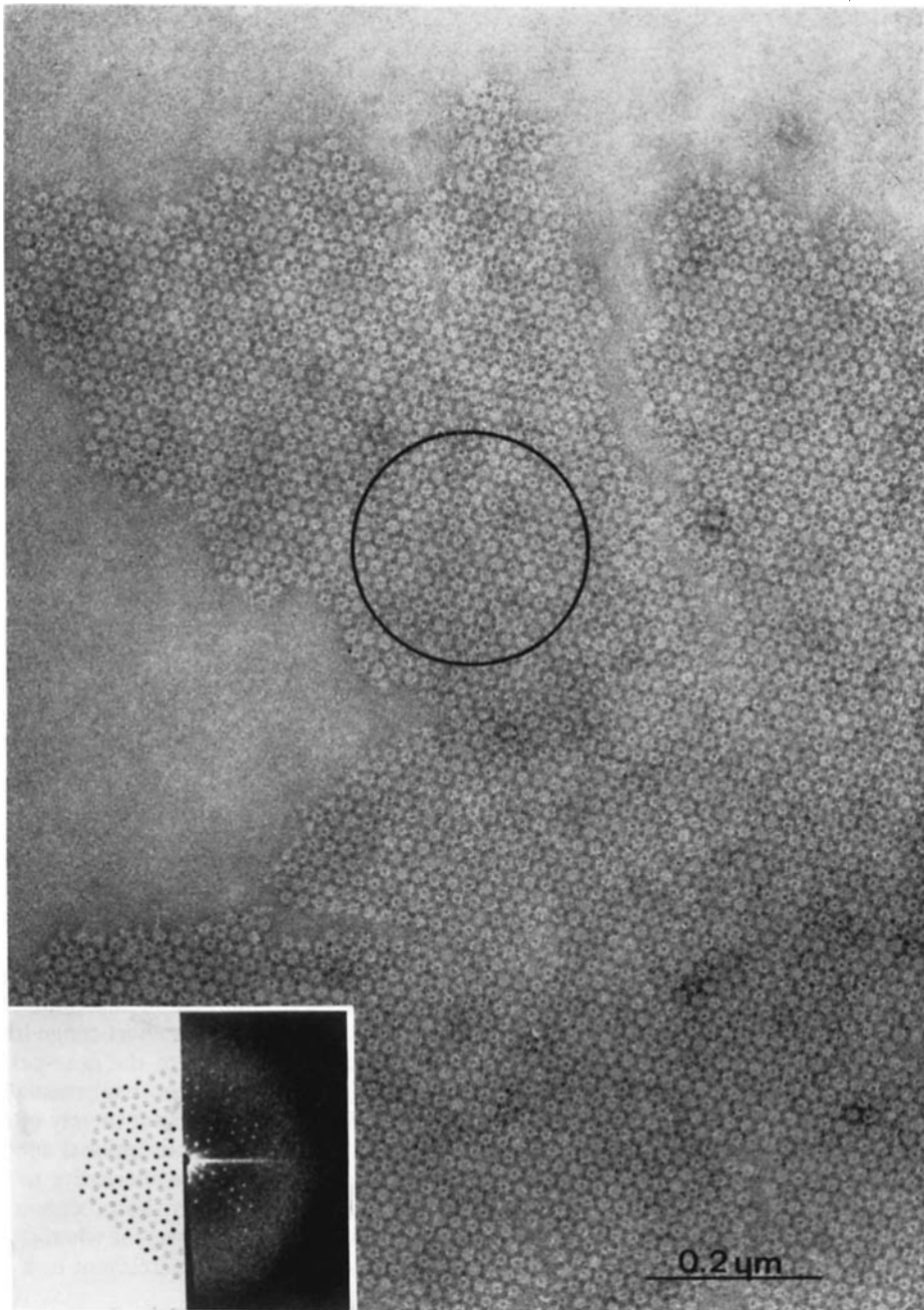


Fig. 1. A sheet of negatively stained HPI-layer showing the typical pattern of centripetal fissures that develop to accommodate the original curvature as the sheet is flattened down on to the support film. The fissures divide the crystal into patches of about 1000 molecules, each separated by regions of presumably high strain. The lattice is hexagonal, with a lattice constant of approximately 18 nm. The encircled area is roughly that used to produce the inset diffraction pattern and the averages presented subsequently. The filled circles in the left half of the diffraction pattern mark those spots with significant intensity in the original.

coherent crystalline patch is sharply limited by the large fissures formed as the layer is forced on to a flat support film (cf. Fig. 1), so that any hope of really high resolution structural information must depend on a method, such as that described here, which is not dependent on crystallinity. The cell wall from which the layer comes is unusually elaborate for a Gram-positive bacterium (Thornley *et al.*, 1965; Work & Griffiths, 1968; Emde *et al.*, 1980). The structure of the HPI-layer, which is a 2-D crystal of naked protein (Baumeister *et al.*, 1982) has been studied extensively with various modes of electron microscopy (Kubler & Baumeister, 1978; Baumeister *et al.*, 1981; Kubler *et al.*, 1980). Correlation with biochemical data requires a higher interpretable resolution however, and this provided the impetus for the present work.

MATERIALS AND METHODS

Micrococcus radiodurans strain R1 (ATCC 13939) was grown at 303 K under aeration in the medium described by Work & Griffiths (1968). HPI-layer sheets were isolated by detergent extraction of whole bacteria as described elsewhere (Baumeister *et al.*, 1982). Electron micrographs of preparations variously negatively stained (sodium silicotungstate and uranyl acetate double staining) and rotary shadowed (Ta/W; angle of incidence 45°, nominal thickness 0.3 nm) were taken in a Siemens Elmiskop 101 under 'low dose' conditions ($< 10^3$ e⁻/nm²) at primary magnifications of approx. 50,000× and 30,000× respectively.

The procedure used to analyse the plates is illustrated diagrammatically in Fig. 2. A small reference area from an image is compared with the whole field, and all the positions of good agreement—whether they fall on a lattice or not—are noted; superposition of all these image positions yields the average, which can then be centred and rotation-symmetrized if desired.

To effect the averaging, two new routines were written for the 'Semper' image processing system (Saxton *et al.*, 1979), and a command procedure was then set up with a number of options/parameters, which was applied in turn to a large number of HPI-layer micrographs, using an IBM 370/165 computer for the averaging runs themselves and a PDP 8/E for initial inspection of the data and final examination of the results. The command procedure requires as data a digitized image area to be processed, a rough value for the lattice constant (~30% or so), the diameter and position of an area of crystal to be used as a 'reference patch' in the correlation process by means of which other similar patches are identified, and the level of rotational symmetry (if any) anticipated in the structure. Given these, the program then embeds the reference patch in an image of the same size as the image to be processed, setting background values to the mean around the perimeter of the reference. It cross-correlates the two arrays, removing very low (less than half the first diffraction order) and very high (more than 0.3 cycles per digitization interval) spatial frequencies by Fourier plane filtration at the same time, so as to make the correlation peaks identifying image regions matching the reference, i.e. unit cell positions, more easily identifiable. A preliminary list of unit cell positions is prepared by locating all local correlation peaks (points at which the eight neighbouring sample values are lower) higher than a detection threshold of 2.5 times the standard deviation in the cross-correlation array, but ignoring any such peaks within a few sample intervals of a previously located peak; these positions are refined by replacing each by the position of the centre-of-mass of a region of the correlation array, one third of a lattice vector in radius, centred at the rough peak position—the purpose being to combat the frequently noisy character of the raw peaks, which often have several local maxima within a single correlation peak. The peak list is sorted into descending order of total 'mass', and two completely independent averages are prepared by superposing image regions (just over two unit cells square) around the odd and even numbered peak positions separately; these are retained for the resolution test described below, and are also combined to form the overall average unit cell image.

If rotational symmetry has been specified, the average is symmetrized accordingly as well as being presented directly. The symmetry axis is located by cross-correlating the average with a rotated copy of itself (180° for P2, P4 or P6 symmetry; 120° for P3) and deducing the original axis position from the displacement of the resulting cross-correlation peak; this approach is mathematically equivalent to the conventional technique of choosing the origin so as to maxi-

mize agreement between the phases of symmetry-related Fourier components, but is rather more efficient. Once the symmetry axis has been located, the rotational average is obtained simply by superposition again.

An option to the procedure, requiring estimates of the lattice vectors (better than $\sim 10\%$ or so) to be supplied with the initial data, provides for an accurate lattice fit to be carried out on the basis of the list of unit cell positions established earlier. The lattice parameters (two base vectors and a vector offset) are determined by minimizing the summed squared deviation be-

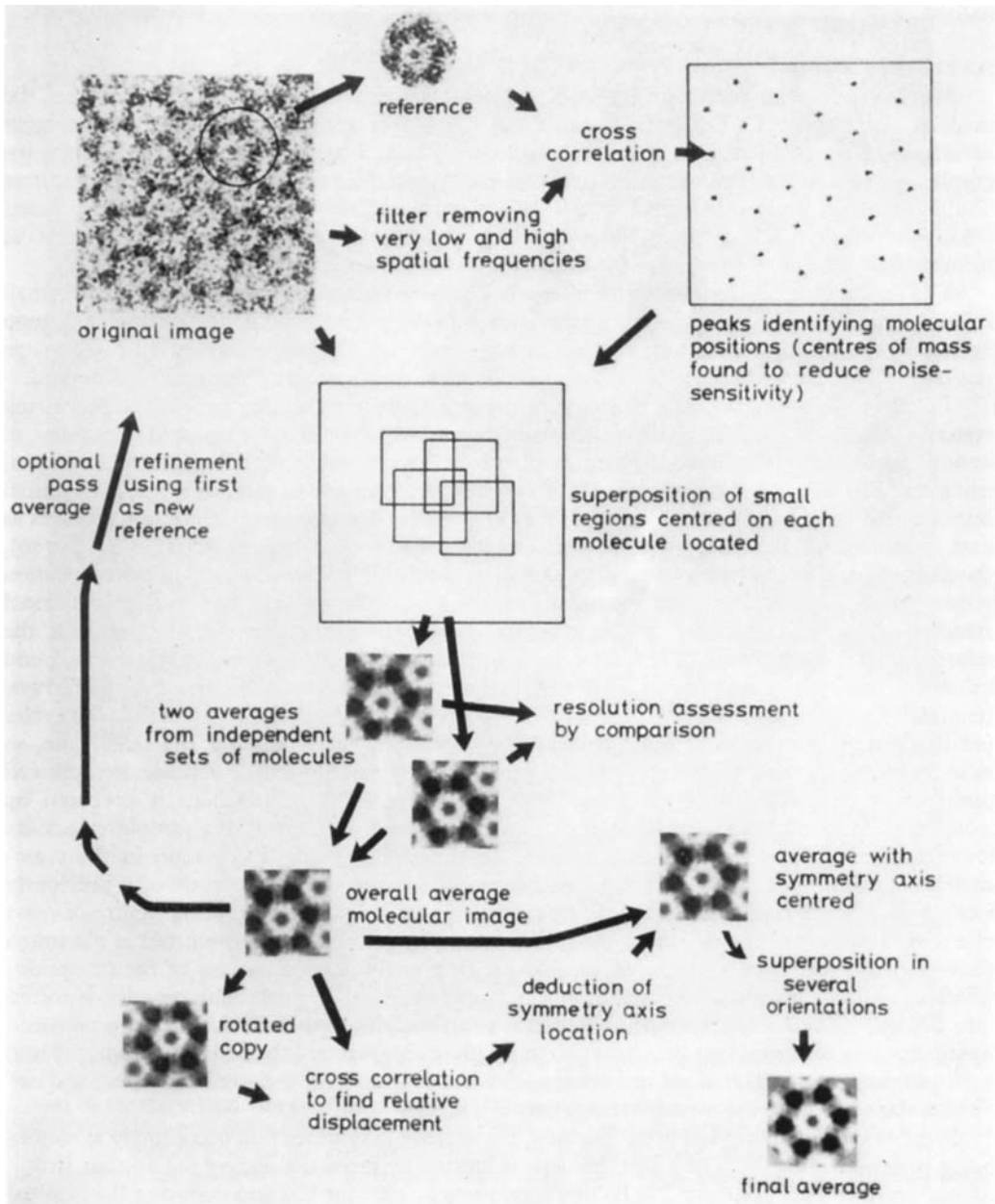


Fig. 2. Schematic illustration of the correlation averaging process, including the optional rotational symmetrization.

tween the unit cell positions and the ideal lattice sites (linear regression); the process requires initial estimates good enough for correct indexing of all positions fitted, and so that this is not inconveniently stringent, the fitting process is carried out three times with progressively larger areas of the image included in the fit. The r.m.s. deviation between the unit cell positions found and the corresponding ideal lattice sites is printed as a convenient measure of the degree of crystal disorder.

For presentation, a region of the average two unit cells square is magnified to 400 points square using bilinear interpolation, and presented with contour lines superposed on a direct grey-level representation; the contour lines are marked in black or white according to whether the underlying image is light or dark, so that they are clearly visible everywhere.

Finally, to provide a resolution assessment, the two independent (odd and even) averages are masked off to a single unit cell, values near the edge of the mask being faded smoothly to a constant background value to prevent artificial high frequency detail, nevertheless common to both averages, from being created at the edge of the mask. The masked averages are transformed and the Fourier components are divided into a number of narrow spatial frequency ranges (width $1/D$ for a unit cell of diameter D), for each of which the cross-correlation coefficient is calculated between corresponding components from the two averages. The purpose is to establish how consistent the two averages are for increasingly fine levels of detail: high correlation for the low frequencies gives place gradually to random fluctuations about zero for high frequencies, so that the first zero crossing provides a simple indication of the reliable resolution limit; the whole curve, which we will here call a 'spatial frequency correlation function', is accordingly plotted for the user to examine subsequently. A similar method using different criteria for the comparison of corresponding Fourier coefficients is described by Frank *et al.* (1981).

An option to the whole procedure allows the average obtained (not rotationally symmetrized) to be used in its turn as a reference for a refinement pass, in which any arbitrary bias in favour of the particular reference chosen originally is eliminated, and the better recognition statistics normally allow a smaller reference to be used, so that lattice distortions are followed more closely.

The automatic procedure above, once established, was applied to a large number of micrographs. The negatively stained and rotary shadowed micrographs under consideration in this paper were digitized at intervals corresponding to 0.51 nm and 0.28 nm respectively; image areas of 512 pixels square (270 unit cells) and 1024 pixels square (350 unit cells) were processed respectively, the reference patch (selected visually) being about 1.5 unit cells in diameter; a refinement pass using the preliminary average as a reference was carried out for the negatively stained micrograph. About 3 min of c.p.u. were needed on the IBM 370/165 computer for the processing of a 512² image.

Further processing was carried out in both cases to test the impression of six-fold rotational symmetry given by the results thus obtained. Firstly, the final average (before symmetrization, of course, but after centring on the supposed symmetry axis) was Fourier transformed, and the real and imaginary parts were displayed separately; also the correlation test applied to the two independent averages to assess the resolution achieved was also applied to a single average and a 60°-rotated copy of itself; the purpose of these two operations are explained in the section that follows.

RESULTS AND DISCUSSION OF THE HPI-LAYER PROTEIN

For brevity, the figures show detailed results only for the negatively stained preparation; no more than the final average is shown for the rotary shadowed case.

Figure 3 shows, for the area of the negatively stained preparation processed, the positions at which molecules were found, and their displacements from ideal lattice positions; the r.m.s. displacements were found to be 0.82 nm in this case and 0.44 nm for the rotary shadowed preparation, which would limit the periodicities recoverable by conventional methods to around 1.6–2.0 nm and 0.8–1.0 nm respectively, given adequate final statistics.

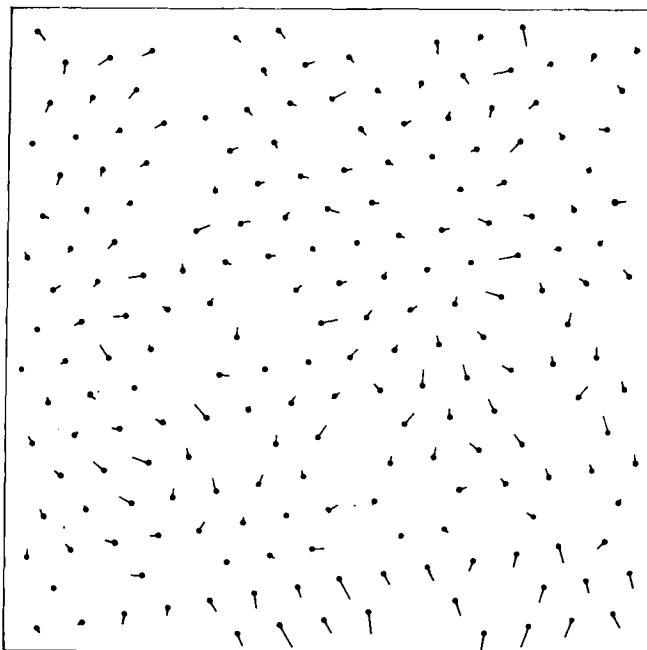


Fig. 3. Molecular positions in a region of the negatively stained preparation. Bold dots mark the positions at which molecules were actually found; small lines emanating from them indicate the direction and distance (magnified 5 times) to the nearest point on a least-squares fitted lattice, thus mapping the displacement field.

Figure 4 shows the independent (odd and even) averages obtained for the negatively stained preparation as well as the cumulative average (before symmetrization); the availability of the two independent averages, exactly aligned, allows a simple and helpful visual assessment of what is signal and what is residual noise in the final average.

Figure 5 is concerned with the assessment of resolution and rotational symmetry. (c) Presents the spatial frequency correlation function between the independent averages in Fig. 4, and indicates for which periodicities the averages contain consistent information; the curve can also be interpreted in terms of the signal-to-noise ratio for the different spatial frequencies, since a correlation coefficient r implies a signal-to-noise power ratio $r/(1-r)$. The broken curve provides a rough threshold level with which to compare the correlation level, being twice the expected standard deviation (i.e. $2/\sqrt{n}$ for n independent Fourier components in a given range—see

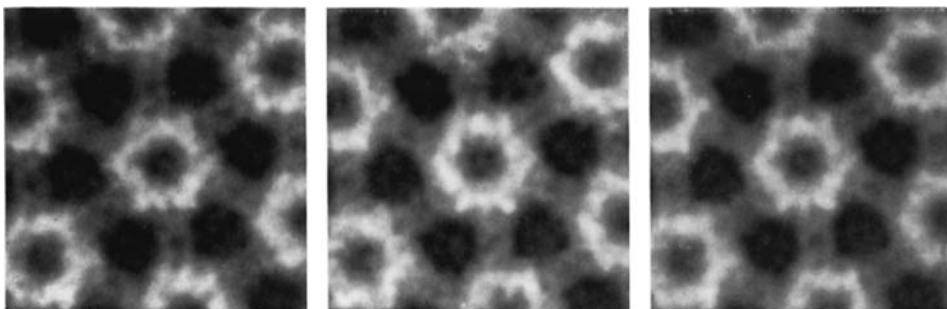


Fig. 4. Averages from the negatively stained preparation. Left and centre: averages obtained from independent sets of molecules; right: cumulative average of these.

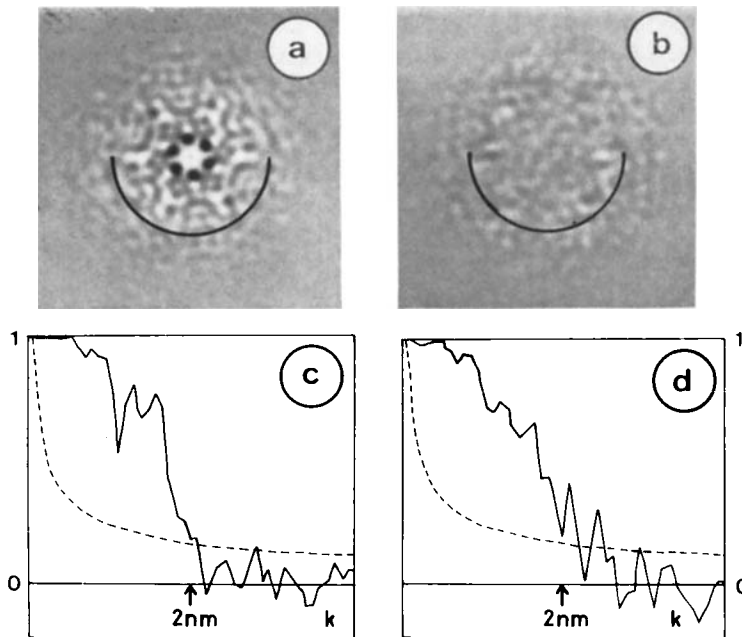


Fig. 5. Resolution and symmetry assessment for the negatively stained preparation. (a) and (b): real and imaginary parts of the Fourier transform of the final average in Fig. 4; the semicircle corresponds to a period of 2 nm; (c): spatial frequency correlation function (correlation coefficient against spatial frequency k) between the two independent averages in Fig. 4; (d): spatial frequency correlation function between the final average and a copy rotated by 60° .

Saxton, 1978, §9.4); the intersection of the two curves (here 1.9 nm) provides a more conservative resolution estimate than the first zero crossing. The other parts of the figure are concerned with testing the impression of six-fold rotational symmetry given by Fig. 3. Firstly, (a) and (b) present the real and imaginary parts of the transform of the final average in Fig. 4—to a consistent grey-scale, but with the real part heavily saturated in any case. P6 symmetry in the specimen would imply P6 symmetry in the real part of the transform, and a zero imaginary part: the symmetry can accordingly be tested by examining (a) and (b) to see whether, and if so to what resolution, these conditions are met; making a reasonable allowance for residual noise present we can see that they are indeed met to the resolution indicated in (c). Lastly, (d) presents the spatial frequency correlation function between the average and the 60° -rotated copy of itself: the similarity of this to the curve in Fig. 5(c) demonstrates that the average agrees as well with itself rotated as it does with an independent average in the same orientation, thus confirming in a rather more objective way the six-fold rotational symmetry of the structure to the resolution obtained. For the rotary shadowed preparation, P6 symmetry was also found, and a resolution of 2.3 nm.

Figure 6, finally, presents rotationally symmetrized and contoured averages from both specimen preparations; it should be noted that the shadowing in the second case is so thin that the protein itself contributes substantially to the contrast observed.

Figures 4 and 6(a) show the core of the HPI-layer protein complex to be made up of two differently sized hexagons (see inset diagram in Fig. 6) skewed against each other by about 25° , though the precise angle varies slightly according to where their boundaries are drawn. Their diameters (measured across the flats) are about 10 nm and 14.5 nm, which agree well with the core dimensions as measured on the two faces (rough and smooth) of the HPI-layer after unidirectional shadowing, which also reveals the two hexagons clearly (Baumeister *et al.*, 1981); this strongly suggests that the larger hexagon is located on the smooth outer surface of the HPI-layer while the smaller hexagon is on the rough inner side. There appear to be twelve morpho-

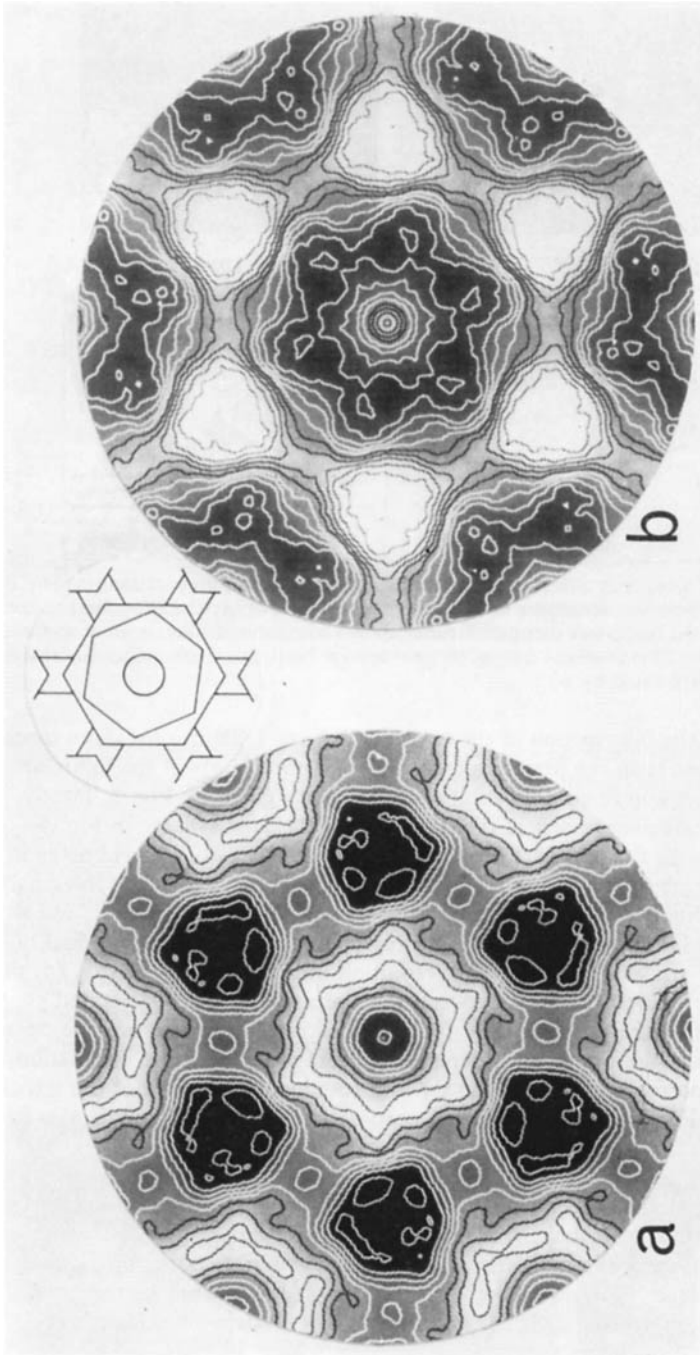


Fig. 6. Six-fold rotationally symmetrized averages of (a) the negatively stained and (b) the rotary shadowed preparation. Contour lines are superposed at intervals of 1% and 1.5% respectively above and below the mean intensity. The small diagram inset draws attention to the two hexagons referred to in the text.

logical subunits (diameter 3–4 nm) in the smaller hexagon, those in the corners more prominent than the interstitial ones. They enclose a central pit (approx. 4.5 nm in diameter)—probably a vestibule narrowing to a transprotein pore; however, no conclusions can be drawn about the shape or smallest diameter of the pore from a projection map. Spokes emanate from the corners of the larger hexagon, interconnecting the cores in the lattice; these spokes are filiform rather than massive structures, dividing the periphery of the core into stain-filled compartments arranged in rosettes.

In the rotary shadowed preparation, Fig. 6(b), in which the statistical definition is somewhat lower, it appears that the build up of shadow at the corners of the small hexagon makes them still more prominent, and the apparent diameter of the hexagon increases slightly, with a corresponding reduction in the skew. The detail visible within the inner hexagon cannot be easily compared with that found in the negatively stained case because of the different contrast mechanism employed; it corresponds well, however, to detail observed in averages from low-dose images of unstained preparations and preparations in which the use of a very small amount of the negative stain accentuates features on the smooth inner surface (Engel *et al.*, 1982). Remarkably, all the fine structure in this lightly shadowed preparation is still visible in subsequent images recorded with substantially higher electron doses.

P6 symmetry is commensurate with biochemical data (Baumeister *et al.*, 1982): the promoters have an apparent molecular weight of 105 kdaltons in SDS-polyacrylamide gel electrophoresis, while direct STEM mass measurements give a total molecular weight close to six times this, namely 650 kdaltons (Kubler *et al.*, 1980). Proteolytic cleavage of the HPI-layer protein, which occurs *in vivo*, complicates the biochemical analysis, but it has now been shown that it does not entail physical disruption of the protein (Rachel *et al.*, 1982).

DISCUSSION OF THE AVERAGING TECHNIQUE

In relation to the single particle averaging procedure described previously, the present application allows a major simplification through the removal of the rotational alignment step and of any need for a preliminary rough location of molecules by hand; these are the crucial factors permitting the present high level of automation which makes the method more convenient as well as more reliable than conventional methods. The refinement of correlation peak positions, through the use of a centre-of-mass determination, leads to greater accuracy in the presence of high noise levels; the methods described for resolution/symmetry assessment address a problem little discussed before—see Frank & Goldfarb (1980) for some suggestions; and the quantification of the disorder in the 2-D crystal also provides information not previously available.

Several observations contribute to our confidence in the reliability of the averages presented. Firstly,—although, following normal practice, we do not reproduce large numbers of averages here—we have now processed about fifty micrographs with the correlation method, and the consistency we have found between averages of independent sets of particles from a single area of crystal, from quite different areas, and even from different preparations sharing common levels of staining and defocus, is highly satisfactory, and much better than was found during the earlier processing of some 150 micrographs by conventional quasi-optical filtration. Similar consistency has been encountered on our varying the diameter of the reference patch chosen, or using the initial average as a fresh reference in its turn. Secondly, the relatively smooth patterns discernible in the displacement map of Fig. 3 and in all other such maps we have examined, imply that the displacements measured are not simply random errors in position determinations. Thirdly, we have obtained extremely close agreement between the displacement map of Fig. 3, which used an arbitrarily selected patch as a reference, and that found when the first average was used as a reference, and are therefore convinced that the accuracy with which molecular positions have been located is, in this case at least, a small fraction of the displacement magnitudes. This improvement in the reliability itself constitutes an effective improvement in resolution, since it allows the interpretation of finer detail in the averages.

We had at first thought it unnecessary to point out in detail all the problems of the con-

ventional techniques, but comments on an earlier draft of this report persuaded us otherwise. The simpler of the two basic conventional approaches is optical filtration, or digital processing mimicking this (e.g. Aebi *et al.*, 1973), in which the average is achieved by 'masking' the Fourier transform of the area to be processed with an array of small windows around the spots: the main problem with this is its sensitivity to the precise size and placing of the windows, obvious to anyone examining the variability of the average from place to place within the filtered image field. Most published results disguise the problem by showing a small arbitrarily selected area only; it stems from the truncation at the edges of the windows of the finite profiles of the diffraction orders—see, e.g., Saxton (1978) §9.6—and prevents fine detail in the average from being interpreted with any real confidence; it is severely compounded, naturally, if the crystal is in any case imperfect.

The alternative conventional approach is the crystallographic one (the basic approach of Unwin & Henderson, 1975, for example), in which the moduli and phases of the diffraction orders are extracted more or less manually by careful examination (or, better, profile fitting) of each order in the transform of the image area to be processed. This is more reliable than optical or quasi-optical filtration, and it is well suited to verifying and/or imposing any symmetry thought to be present, and to exploiting any additional data available (such as electron or X-ray diffraction patterns), though it is obviously much more time-consuming to perform, being therefore less widely practised. Its results too are, however, somewhat ambiguous in many instances: it is popularly but incorrectly supposed, for instance, that the visibility of a spot in an optical or digital diffractogram is sufficient for useful information at the corresponding periodicity to be available in the final average; in practice it is often found that the phase varies too rapidly and irregularly across a diffraction spot profile for any reliable value to be determined for the phase, so that any contribution the spot is allowed to make to the final average can be no more than pure guesswork. The limited reliability of the phases found is also made clear by the frequent failure of *all* diffraction orders to share the symmetry finally assigned (by majority vote, as it were) to a structure. Now this kind of phase instability within a diffraction order is of course precisely what is expected in the presence of long-range crystal imperfections, and the correlation approach to averaging is the only way so far proposed of combatting it.

P. R. Smith's intermediate method (Aebi *et al.*, 1973) in which, after an initial diffractogram calculation to establish the lattice parameters, the image is re-sampled digitally on a sampling lattice exactly commensurate with the crystal lattice, so that the diffraction orders—given perfect crystallinity—are no longer of finite width, is a convenient way of evading the worst problems of the quasi-optical approach without involving the greater effort of the crystallographic method; where the spot profiles are degraded by imperfect crystallinity however, this regular re-sampling cannot of course improve them. Crowther & Sleytr (1977), in their early attempt to correct for lattice distortions, adopt a re-sampling that varies from cell to cell so as to follow the distortions, an approach that does of course offer real improvement in principle. The limitation of their method was the lack of a convenient automatic means of determining the pattern of re-sampling required—they relied on heavy low pass filtering to make unit cell positions clear (at this stage deliberately discarding all the higher resolution information, of course), and then transcribed the resulting distortion pattern by hand.

In the present case, the r.m.s. molecular displacements found mean that imperfect crystallinity has not in fact been the limiting factor, which is more likely to have been the extent to which the contrast enhancing media are able to portray the precise boundary of the protein. Nevertheless, the use of the correlation averaging method instead of conventional methods has allowed a more detailed interpretation of the average with greater confidence, in spite of a substantially higher rate of throughput. In other cases, other benefits can be expected. When poor image noise statistics are the limiting factor, such as in minimum dose microscopy of unstained preparations, the correlation method can be used to extend an average evenly over all the molecules in many crystal fragments, even when as here the fragments have highly irregular shapes, the procedure being adjusted somewhat to allow for differences in orientation and defocus between fragments (Saxton, 1980; Engel *et al.*, 1982).

The principal importance of correlation averaging is obviously, however, its ability to compensate for lattice distortions where these are the limiting factor (e.g. Kuhlbrand & Unwin, 1980), and the treatment of these distortions bears further comment. Varying molecular displacements of course imply some distortion (strain) of individual molecules as well; the procedure as described above makes no attempt to compensate for these, and the fact evinced by Fig. 3 that the displacements normally relax over several molecules offers some justification for this. We can, however, take advantage of the knowledge of the displacement field which the method provides to eliminate the problem altogether, by selecting for averaging only those molecules in low strain (not necessarily low displacement) areas where molecular distortions may reasonably be assumed to be least; the first results from such an approach have already been reported (Saxton & Baumeister, 1981). Selective averages might be prepared according to different criteria too, of course, the most obvious being the correlation peak height—i.e. including only those which correlate most strongly with the reference; however, since the reference would have to be a preliminary average, so as to avoid any arbitrary bias, it does not seem likely that it would in fact be very successful in recognizing the 'best' molecules preferentially; with the present data, we found that the degradation of the noise statistics arising from using only 30% or so of the molecules present more than offset any benefit due to the selectivity of the average. Correspondence analysis (van Heel & Frank, 1981) offers a much more sophisticated approach to selection, since it provides an objective and automatic, though not yet rapid, way of detecting and classifying systematic differences within a population of molecules. It is clearly at its most powerful in recognizing discrete differences in molecular characteristics, but could also be of some value in the context of the more continuous differences anticipated here.

Patently, a 3-D structure is required in due course for the HPI-layer as it is for any 2-D crystal, as this will allow a far more detailed correlation between morphology, biochemistry and function than a single projection permits. Again, comments made to us have shown that it is in fact necessary to point out that correlation averaging is as capable of leading to a 3-D structure as are conventional methods, since either approach provides in the first instance well-defined projections as one chooses, from which a 3-D structure can be deduced subsequently by any of the several well-established methods; work in this direction is currently in hand. The search for higher resolution evidently requires a sacrifice of contrast and a resort to alternative less convenient specimen preparation techniques not themselves imposing such stringent resolution limits; work is also in progress with freeze-dried unstained, and aurothioglucose embedded, preparations exploiting more fully the advantages of the correlation averaging method.

ACKNOWLEDGMENTS

We wish to thank Dr R. A. Crowther for densitometering some of the micrographs contributing to this paper, and Mrs G. Flaskamp for excellent technical assistance. The financial assistance of the Deutsche Forschungsgemeinschaft (Sonderforschungsbereich 160), the U.K. Science Research Council and the European Molecular Biology Organization is acknowledged.

REFERENCES

- Aebi, U., Smith, P.R., Dubochet, J., Henry, C. & Kellenberger, E. (1973) A study of the structure of the T-layer of *Bacillus brevis*. *J. supramolec. Struct.* **1**, 498.
- Baumeister, W., Karrenberg, F., Rachel, R., Engel, A., ten Heggeler, B. & Saxton, W.O. (1982) The major cell envelope protein of *Micrococcus radiodurans* (R1): structural and chemical characterization. *Eur. J. Biochem.* (in press).
- Baumeister, W., Kubler, O. & Zingsheim, H.P. (1981) The structure of the cell envelope of *Micrococcus radiodurans* as revealed by metal shadowing and decoration. *J. Ultrastruct. Res.* **75**, 60.
- Crowther, R.A. & Sleytr, U.B. (1977) An analysis of the fine structure of the surface layers from two strains of *Clostridia*, including correction for distorted images. *J. Ultrastruct. Res.* **58**, 41.
- Engel, A., Saxton, W.O. & Baumeister, W. (1982) Mass mapping of a protein complex with the STEM. *Proc. nat. Acad. Sci. U.S.A.* (in press).
- Emde, B., Wehrli, E. & Baumeister, W. (1980) The topography of the cell wall of *Micrococcus radiodurans*. In: *Proc. 7th Eur. Cong. EM, The Hague* (Ed. by P. Brederoo and W. de Priester), Vol. 2, p. 460.

- Frank, J. (1980) Correlation averaging applied to micrographs of crystalline cytochrome oxidase. In: *Proc. 7th Eur. Cong. EM, The Hague* (Ed. by P. Brederoo and W. de Priester), Vol. 2, p. 694.
- Frank, J. & Goldfarb, W. (1980) Methods for averaging of single molecules and lattice-fragments. In: *Electron Microscopy at Molecular Dimensions* (Ed. by W. Baumeister and W. Vogell), p. 261. Springer, Berlin.
- Frank, J., Goldfarb, W., Eisenberg, D. & Baker, T.S. (1978) Reconstruction of glutamine synthetase using computer averaging. *Ultramicroscopy*, **3**, 283.
- Frank, J., Verschoor, A. & Boublik, M. (1981) Computer averaging of electron micrographs of 40S ribosomal subunits. *Science*, **214**, 1353.
- van Heel, M. & Frank, J. (1981) Use of multivariate statistics in analysing the images of biological macromolecules. *Ultramicroscopy*, **6**, 187.
- Kubler, O. & Baumeister, W. (1978) The structure of the periodic cell wall component (HPI-layer) of *Micrococcus radiodurans*. *Cytobiologie*, **17**, 1.
- Kubler, O., Engel, A., Zingsheim, H.P., Emde, B., Hahn, M., Heisse, W. & Baumeister, W. (1980) Structure of the HPI-layer of *Micrococcus radiodurans*. In: *Electron Microscopy at Molecular Dimensions* (Ed. by W. Baumeister and W. Vogell), p. 11. Springer, Berlin.
- Kuhlbrand, W. & Unwin, P.N.T. (1980) Structural analysis of stained and unstained two-dimensional ribosome crystals. In: *Electron Microscopy at Molecular Dimensions* (Ed. by W. Baumeister and W. Vogell), p. 108. Springer, Berlin.
- Rachel, R., Engel, A. & Baumeister, W. (1982) Proteolysis of the major cell envelope protein of *Micrococcus radiodurans* occurs *in vivo* but remains morphologically latent. *FEBS Letters* (in press).
- Saxton, W.O. (1978) *Computer Techniques for Image Processing in Electron Microscopy*. Academic Press, New York.
- Saxton, W.O. (1980) Matching and averaging over fragmented lattices. In: *Electron Microscopy at Molecular Dimensions* (Ed. by W. Baumeister and W. Vogell), p. 245. Springer, Berlin.
- Saxton, W.O. & Baumeister, W. (1981) Image averaging for biological specimens: the limits imposed by imperfect crystallinity. In: *Developments in Electron Microscopy and Analysis 1981* (Ed. by M. J. Goringe), p. 333. Institute of Physics, Bristol.
- Saxton, W.O. & Frank, J. (1977) Motif detection in quantum noise limited electron micrographs by cross-correlation. *Ultramicroscopy*, **2**, 219.
- Saxton, W.O., Pitt, T.J. & Horner M. (1979) Digital image processing: the Semper system. *Ultramicroscopy*, **4**, 343.
- Sleytr, U.B. (1978) Regular arrays of macromolecules on bacterial cell walls: structure, chemistry, assembly and function. *Int. Rev. Cytol.* **53**, 1.
- Thornley, M.H., Horne, R.W. & Glauert, A.M. (1965) The fine structure of *Micrococcus radiodurans*. *Arch. Microbiol.* **51**, 267.
- Unwin, P.N.T. & Henderson, R. (1975) Molecular structure determination by electron microscopy of unstained crystalline specimens. *J. molec. Biol.* **94**, 425.
- Work, E. & Griffiths, H. (1968) Morphology and chemistry of the cell wall of *Micrococcus radiodurans*. *J. Bacteriol.* **95**, 641.